J Mater Sci (2006) 41:5915–5925
DOI 10.1007/s10853-006-0278-2

Thermal, mechanical and vibration characteristics of epoxy-clay nanocomposites

T. P. Mohan · M. Ramesh Kumar · R. Velmurugan

Received: 2 June 2005 / Accepted: 18 October 2005 / Published online: 6 July 2006

Abstract Diglycidyl ether of bisphenol-A (DGEBA) epoxy resin system filled individually with organoclay (OC) and unmodified clay (UC) were synthesized by mechanical shear mixing with the addition of diaminodiphenylmethane (DDM) hardener. The unmodified clay used was Na^+-Montmorillonite (MMT) and the organoclay was alkyl ammonium treated MMT clay. The reinforcement effect of OC and UC in the epoxy polymer on thermal, mechanical and vibration properties were studied. X-ray diffraction (XRD) and Transmission electron microscopy (TEM) were used to study the structure and morphology of nanocomposites. Curing study shows that the addition of OC in epoxy resin aids the polymerization by catalytic effect, and UC addition does not show any effect in the curing behavior of epoxy polymer. Thermogravimetry analysis (TGA) shows enhanced thermal stability for epoxy with OC fillers than that of epoxy with UC fillers. The epoxy with OC fillers shows considerable improvement on tensile and impact properties over pure epoxy polymer and epoxy with UC fillers. The improvement in tensile and impact properties of nanocomposites is supported with the fracture surface studies. Epoxy with OC fillers shows enhanced vibration characteristics than that of the pure epoxy polymer and epoxy with UC fillers.

T. P. Mohan · M. R. Kumar · R. Velmurugan (✉)
Composites Technology Centre, Indian Institute of Technology Madras, Chennai 600 036, India
e-mail: rvel@iitm.ac.in

Introduction

Polymers filled with nano-layered silicate clay particles have attracted researchers in the recent years due to their superior mechanical (tensile, impact, etc.), thermal (decomposition, mass loss, etc.) and physical (barrier, optical, etc.) properties. Such improved properties were noted at small filler content (< 5 wt.%) in the polymer matrix with very little change in density [1–4]. Montmorillonite clay was widely used as reinforcement filler in polymer matrix due to its chemical compatibility with matrix polymer. The MMT is a 2:1 phyllosilicate crystal structure consisting of two silica tetrahedral sheets sandwiching an edge shared octahedral sheet. Aluminium or magnesium hydroxyl isomorphous substitutions of Si^{4+} for Al^{3+} in the tetrahedral lattice and of Al^{3+} for Mg^{2+} in the octahedral lattice cause an excess of negative charges within the MMT layer. These negative charges are counterbalanced by cations such as Ca^{2+} and Na^+ situated between the layers. Stacking of layers leads to regular van der Waals gap called interlayer or galleries. The interlayer represents the repeated unit of the multilayer material, and the distance between each layer is called d-spacing or basal spacing, and is calculated from the (001) harmonics from X-ray diffraction patterns. Each layer is very thin (1 nm) and length varies from 100 nm to 1000 nm. MMT clays are hydrophilic in nature, and to render them organophilic (compatible with organic polymers), exchangeable ions that are situated at the interlayer of MMT clay are replaced by organophilic ions such as alkyl ammonium ions. The exchange is carried by cation exchange process. The ease of chemically exchangeable and availability makes MMT clay a superior nano filler than other clays. This organophillic clay is called as organoclay (OC), and when they are added in to the matrix polymer, it will lead to the

dispersion of individual nano layers in the matrix. The dispersion of nano layers is absent when unmodified MMT is added in the polymer matrix, and this leads to the conventional micron-scale particle filled composites [5–8]. In general, addition of clays in the polymer matrix leads to three different types of structures. First, a phase separated clay and polymer in which the clay acts as conventional filler in the polymer matrix. Second, the intercalated structure, in which the clay layers are separated due to the presence of matrix polymer in the interlayer, and still regular parallel arrangement of layers is maintained. Third, the exfoliated structure, in which the clay layers are randomly distributed in the matrix polymer. The intercalated and exfoliated structures are seen when OC is added in to the polymer. The unmodified MMT clay addition leads to the conventional composites. The exfoliated structure possesses superior properties among the three existing structures. The high surface contact area of matrix polymer to nanolayers, uniform distribution of nano layers, etc. of exfoliated structure enhance the properties than other two structures [9–11].

Thermoset epoxy-clay nanocomposites (ECN) are studied under different curing conditions, synthetic routes, organoclays, etc. The report suggests that good exfoliation can be achieved in ECN when amine based curing agents are used [11–16]. The reactants of epoxy systems have a suitable polarity to diffuse between the clay layer and form an exfoliated nanocomposite upon polymerization. The alkyl ammonium ions of OC that are at the gallery region generate protons and then attack the epoxy ring, causing acid catalysed ring opening homopolymerization. The ammonium ions of OC polymerize the epoxy resin that are at the interlayer gallery region, and as the curing progresses further the interlayer space is increased due to more entry of polymer matrix in the gallery region. If the curing rates inside and outside clay layers are comparable, then it favours the formation of exfoliated structure [17–20]. Although several types of amine curing agents are available in the literature, limited reports are available on diaminodiphenyl methane (DDM) curing agent [11]. The DDM curing agent is widely used for making glass fibre reinforced epoxy composites. The main purpose of nanoclay filler is to increase the matrix properties of fibre reinforced polymer composites. The addition of nanoclay in epoxy resin with addition of DDM curing agent is an important phenomenon to consider as large amount of glass fibre reinforced composites are used in several applications. In this work, the effect of organo modified MMT clay and unmodified MMT clay addition in the epoxy polymer matrix, under DDM curing is studied. The curing behaviour, structure, tensile, thermal and vibration properties are studied for various clay concentrations.

Experimental details

Materials

The matrix material used in this present system is DGEBA epoxy resin system and the curing agent is diaminodiphenyl methane (DDM), both obtained from CIBA Ltd, Basle (Switzerland). The reinforcement fillers in matrix are unmodified Na^+-Montmorillonite clay and an organoclay. The organoclay is alkyl ammonium clay obtained from Southern Clay Products Ltd, Gonzalez, Texas (USA).

Nanocomposite fabrication

Initially epoxy resin is heated at 120 °C for 1 h. The clay is then gently added in to the resin bath. Mixing of clay and epoxy is carried out by mechanical shear mixer. The mixer rotates at 1000 rpm and mixing is carried out for 2 h. After uniform mixing of clay and resin, DDM hardener is added in to the resin–clay solution. The resin to hardener ratio is maintained 4:1, and then is casted in the mold. The mold is kept at 80 °C for 4 h until complete polymerization occurs. The nanocomposite specimens synthesized by this method are tested for various characterizations.

Characterization

Curing characteristics of epoxy and epoxy filled OC and UC series is studied using DSC. The sample (consisting of resin, clay and hardener prior to curing) of 5 mg is taken in an alumina crucible and heat is applied at the rate of 10 °C/min. XRD is performed to evaluate the degree of intercalation/exfoliation of nanocomposites. XRD is carried out with a scanning rate of 2 °/min with CuKα radiation (λ = 1.5401 Å) operating at 30 KV and 15 mA. Thin sections of sample are made for TEM-Philip electron microscopy operating at 200 KV. Thermogravimetry analysis (TGA) is carried out using Netzsch Model STA 409 PC. Samples of 5 mg are taken in alumina crucible for TGA test and heat is applied to the sample at the rate of 10 °C/min. Tensile testing is carried out using Instron machine at a cross-head speed of 1 mm/min according to ASTM D638. Izod un-notched impact testing is carried out according to ASTM D256. Fracture surfaces of tensile and impact tested specimens are carried out by using Scanning Electron Microscope (SEM). Modal analysis is performed to calculate natural frequency and damping factor 'ξ'. Damping factor is calculated using Impulse Hammer Technique (IHT) and Logarithmic Decrement Method (LDM). A Nanocomposite specimen of 250 × 25 × 3 mm is prepared, in which one end of beam is clamped and other end is attached to accelerometer to obtain vibration modes. Natural frequency is determined by impulse loading at free

end of the bean using impulse exicitation (Rion PH 7117, modally tuned hammer). The signal received from accelerometer is displayed in Fast Fourier Transform (FFT), in which natural frequency is noted down for various modes. Damping factor 'ξ' using IHT is determined using half-power bandwidth method. The expression for damping factor by half power width technique is given by $\xi = (\Delta\omega/2\omega_n)$, where $\Delta\omega$ is bandwidth at half-power points of resonant peak for the nth mode and ω_n is resonant frequency. The half power points are found at $[1/\sqrt{2}]$ of maximum peak value.

In the LDM, sine wave signal is supplied to drive the modal exciter to excite the cantilever beam specimen. During the natural frequency mode, the amplitude increases to a large extent, once the resonance is achieved. At this point, the excitation signal is disconnected freely and a typical free decay curve is obtained. From this decay curve, two experimental amplitude data points are collected namely x_1 and x_{n+1} , and the damping factor ξ is calculated by using the expression

$$\delta = \frac{1}{n+1}\ln\frac{x_1}{x_{n+1}}$$

$$\zeta = \frac{\delta^2}{\sqrt{4\pi^2+\delta^2}}$$

where ξ, the damping factor, $n + 1$, the number of cycles, δ is the logarithmic decrement, x_1 and x_{n+1} are the two displacement values at the time intervals t_1 and t_2, respectively.

Results and discussion

Curing characteristics

DSC scans of epoxy, epoxy filled with OC and epoxy filled with UC clay are shown in Fig. 1. Pure epoxy shows a single exothermic peak at 160 °C. At 1 wt% OC addition, the peak position has decreased to lower temperature as shown in Fig. 1a. At higher clay content (>3 wt% OC), two distinct peaks are noticed, one at lower temperature and another at higher temperature. The higher temperature peak is noticed at curing peak of pure epoxy resin. The lower temperature peak corresponds to curing of epoxy resin in intergallery region, and higher temperature peak corresponds to curing at extragallery (matrix) region. As clay content increases above 3 wt% the lower temperature peak decreases and for 10 wt% OC it is at 119 °C. Single exothermic peak is noted for epoxy with OC content up to 2 wt% OC and results in uniform polymerization. This uniform polymerization at intergallery region and extragallery (matrix) region could have favored the exfoliated structure. At higher OC content (>3 wt%), the uneven polymerization occurs in the nanocomposites and this leads to two distinct curing exothermic peaks. The intergallery polymerization occurs at lower temperature and cures quicker than that of the extragallery polymerization. Due to this quick intergallery polymerization, the clay nanolayers cannot separate further. This uneven polymerization leads to the formation of intercalated nanocomposite structure for higher OC content (above 3 wt%). The DSC curing scans of epoxy and epoxy filled with UC are shown in Fig. 1b. It is seen that the addition of UC does not shift the exothermic peak, which is noted for OC contents. The result suggests that addition of UC fillers in epoxy resin does not affect the curing of epoxy. The addition of OC and UC fillers in the epoxy decreases the intensity of exothermic peak. The clay addition continuously decreases the exothermic peak and this is due to decrease in concentration of epoxy resin on clay addition. It is stated that the presence of organo ions in OC increases the polymerization of epoxy by catalytic effect [21] and has to increase the curing temperature. However, the existence of nanolayers affects the polymerization of epoxy. Results show that the effect of nanolayers restricting the polymerization is more than the polymerization of organo ions with epoxy polymer, and hence decreases the curing temperature of epoxy resin.

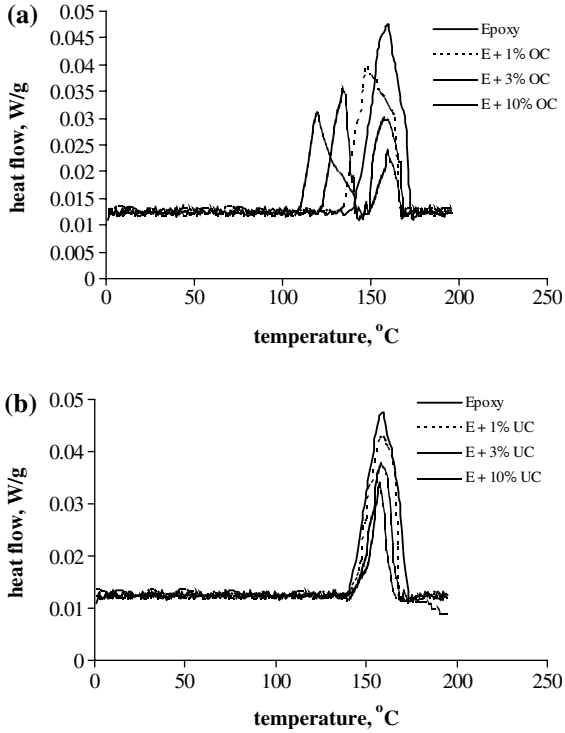

Fig. 1 DSC scans of (**a**) epoxy with OC series (**b**) epoxy with UC series

Structure and morphology of nanocomposites

The XRD pattern of organoclay and unmodified clay is seen in Fig. 2a. The peak occurred at 5.2 ° and 6.62 ° for OC and UC, respectively. The interlayer spacing (d-spacing) of OC and UC is 17 Å and 13.3 Å, respectively. It is observed that interlayer spacing of OC is higher than that of UC. The presence of alkyl ammonium ions at gallery region has increased the interlayer spacing of OC than UC. XRD pattern of epoxy filled with OC particles is seen in Fig. 2b. It is observed that up to 2 wt% OC, the basal spacing reflection of OC is absent. This indicates that exfoliated nanocomposite structure has formed, or interlayer distance of clay is above 75 nm in which Bragg's law does not obey [22]. For higher OC addition (>3 wt%), sharp reflection peak is noticed which indicates that intercalated nanocomposite structure has formed. The peak reflection is obtained at 3 °, 3.1 ° and 3.3 ° for 3%, 5% and 10% of OC content in epoxy matrix. The interlayer spacing is 30.43 Å and 26.74 Å for 3% and 10% of OC content in epoxy matrix. XRD pattern of epoxy filled with UC particles is seen in Fig. 2c. It shows a sharp peak for all the epoxy filled UC series. The reflection peak is obtained at same basal reflection peak of UC. This shows that clay nanolayer

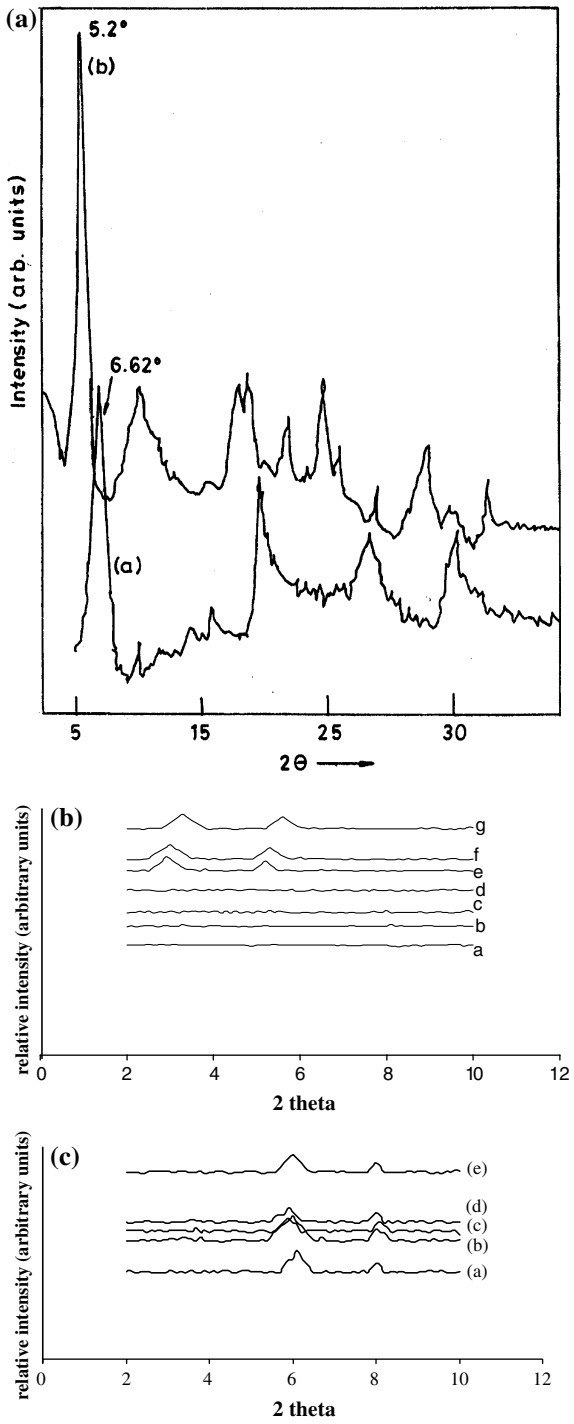

Fig. 2 XRD pattern of clay, epoxy with OC and UC series. (**a**) XRD pattern of (a) organoclay and (b) unmodified Montmorillonite clay. (**b**) XRD pattern of epoxy with (a) 0.5% OC, (b) 1% OC, (c) 1.5% OC, (d) 2% OC, (e) 3% OC, (f) 5% OC and (g) 10% OC. (**c**) XRD pattern of epoxy with (a) 1% UC, (b) 2% UC, (c) 3% UC, (d) 5% OC and (e) 10% UC.

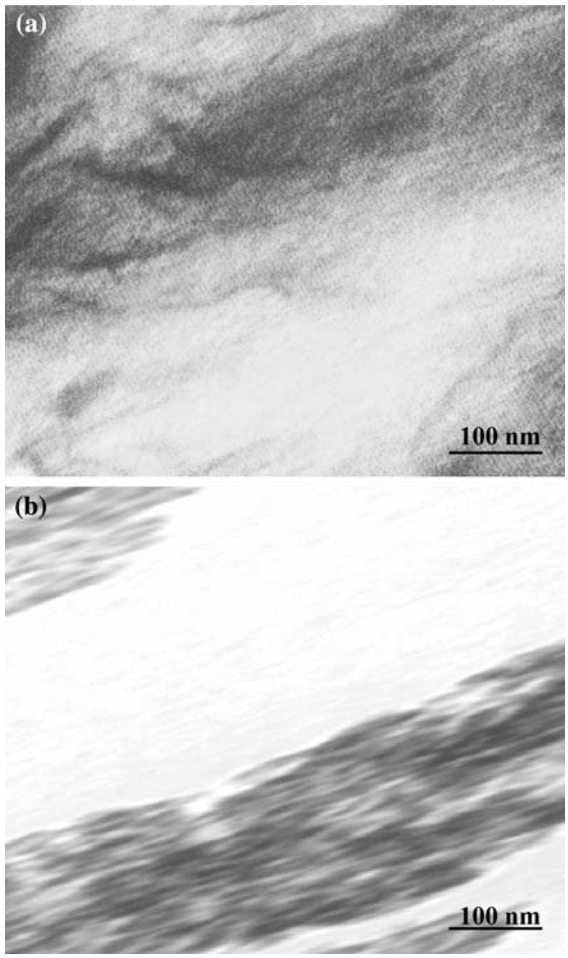

Fig. 3 TEM of epoxy with (**a**) 2% OC and (**b**) 10% OC

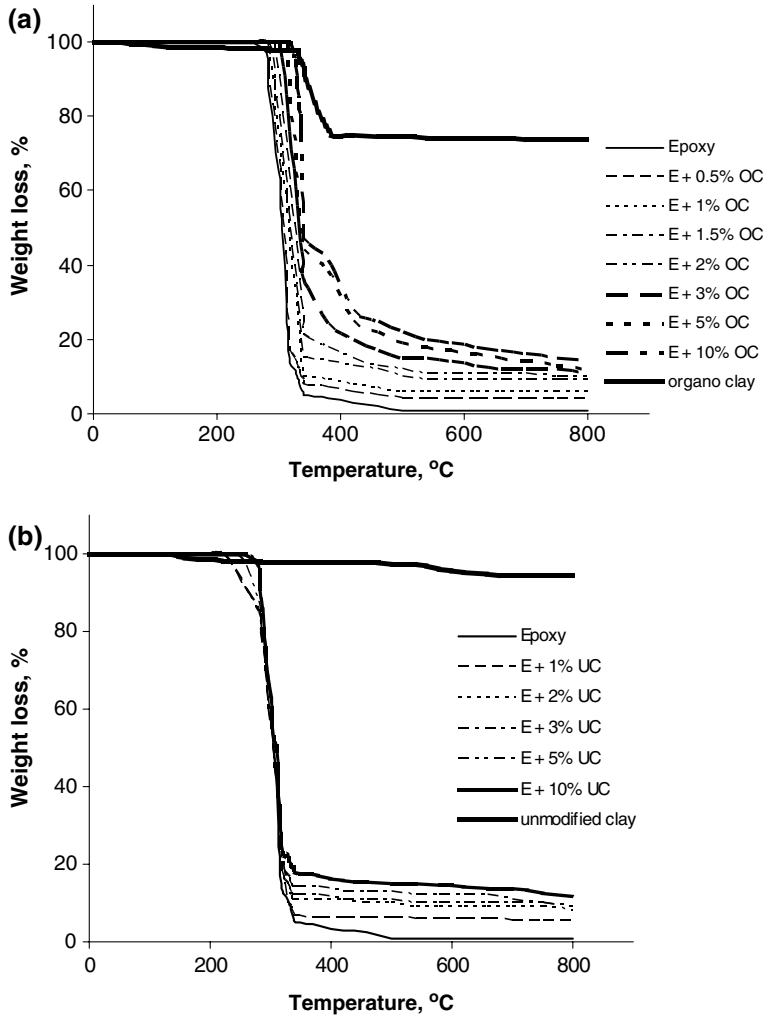

Fig. 4 TGA thermograms of epoxy with (**a**) OC series and (**b**) UC series

separation is absent in epoxy polymer, and UC clay acts as conventional micron scale particle filled composites.

Figure 3 shows TEM of epoxy filled with 2% and 10% of OC particles. It is seen that at lower clay content, clay nanolayers are well separated and has formed exfoliated nanocomposite structure. At higher clay content (10%), intercalated nanocomposite structure has formed.

Thermogravimetry analysis [TGA]

Figure 4 shows TGA of epoxy, organoclay, epoxy filled with OC and epoxy filled with UC particles. The TGA curve shows the decomposition of epoxy, epoxy with OC and epoxy with UC. Figure 4a shows decomposition of OC at 335 °C and is due to dissociation of alkyl ammonium ions. Pure epoxy decomposition starts at 280 °C. On addition of OC in epoxy polymer, the decomposition starts at higher temperature. In epoxy with 10% OC, decomposition starts at 324 °C. The hard nanolayers act as barrier for volatile degradation of polymer matrix. This effect causes such enhanced thermal properties for nanocomposites. The enhanced thermal stability of nanocomposites is noted even at higher temperature (>400 °C). At this high temperature (>400 °C), the existence of inorganic phases (SiO_2, Al_2O_3, MgO, etc.) [23] dominates the nanocomposites and cause such enhanced thermal stability.

Figure 4b shows decomposition of UC, epoxy and epoxy filled UC particles. The UC shows negligible decomposition up to 800 °C. The addition of UC particles does not improve the decomposition of epoxy polymer. There is a marginal shift in decomposition temperature when UC is added in to the epoxy polymer. The improved thermal stability is noticed for epoxy filled UC series at higher temperatures (>400 °C). The reinforcement of OC increases the decomposition of epoxy. The UC addition does not show any improvement in decomposition of epoxy polymer.

Tensile properties

The stress–strain curves for epoxy with OC and UC series under uniaxial tension are shown in Fig. 5. Figure 6 shows the effect of clay addition on tensile strength (Fig. 6a) and tensile modulus (Fig. 6b). The addition of clay on epoxy has considerable effect in the stress–strain behavior as is seen from Fig. 5. The tensile strength of pure epoxy is 61.1 MPa. The tensile strengths of organoclay filled epoxy are 64.5 MPa, 66 MPa, 64.67 MPa, 61.62 MPa and 61.5 MPa for 1%, 2%, 3%, 5% and 10% of OC, respectively. It is seen that tensile strength increases up to 2 wt% of OC addition in epoxy polymer matrix. As the OC content increases further (>2%), strength decreases. Epoxy with 10% of OC, strength is 61.5 MPa but above the strength of pure epoxy polymer matrix. The formation of exfoliated nanocomposite structure up to 2% OC increases the strength of nanocomposites. The formation of intercalated structure, agglomeration, presence of voids, etc., above 2% OC have decreased the strength of the nanocomposites. The addition of UC decreases the tensile strength of epoxy material. Tensile strengths of unmodified clay filled epoxy are 62.58 MPa, 60.2 MPa, 57.76 MPa, 55.8 MPa and 52.82 MPa for 1%, 2%, 3%, 5% and 10% of UC, respectively. It is seen from Fig. 5 that addition of clay decreases the strain at break. The low strain value is due to the formation of voids, agglomeration, etc. The effect of OC and UC addition on tensile modulus is seen in Fig. 6b. Tensile modulus of pure epoxy is 2.9 GPa. On addition of OC, tensile modulus increases to 3.48 GPa, 3.84 GPa, 4.1 GPa, 4.33 GPa and 4.41 GPa for 1%, 2%, 3%, 5% and 10% of OC, respectively. It is observed that modulus of nanocomposites increases continuously with increasing OC clay content. An improvement in modulus of ~1.5 times is observed for the addition of 10% OC. The orientation of clay platelets and polymer chains with respect to loading direction can also contribute to reinforcement effects. The decreasing rate of modulus at higher clay content (>2% OC) is due to presence of unexfoliated aggregates in epoxy polymer matrix. In epoxy–UC composites, there is not

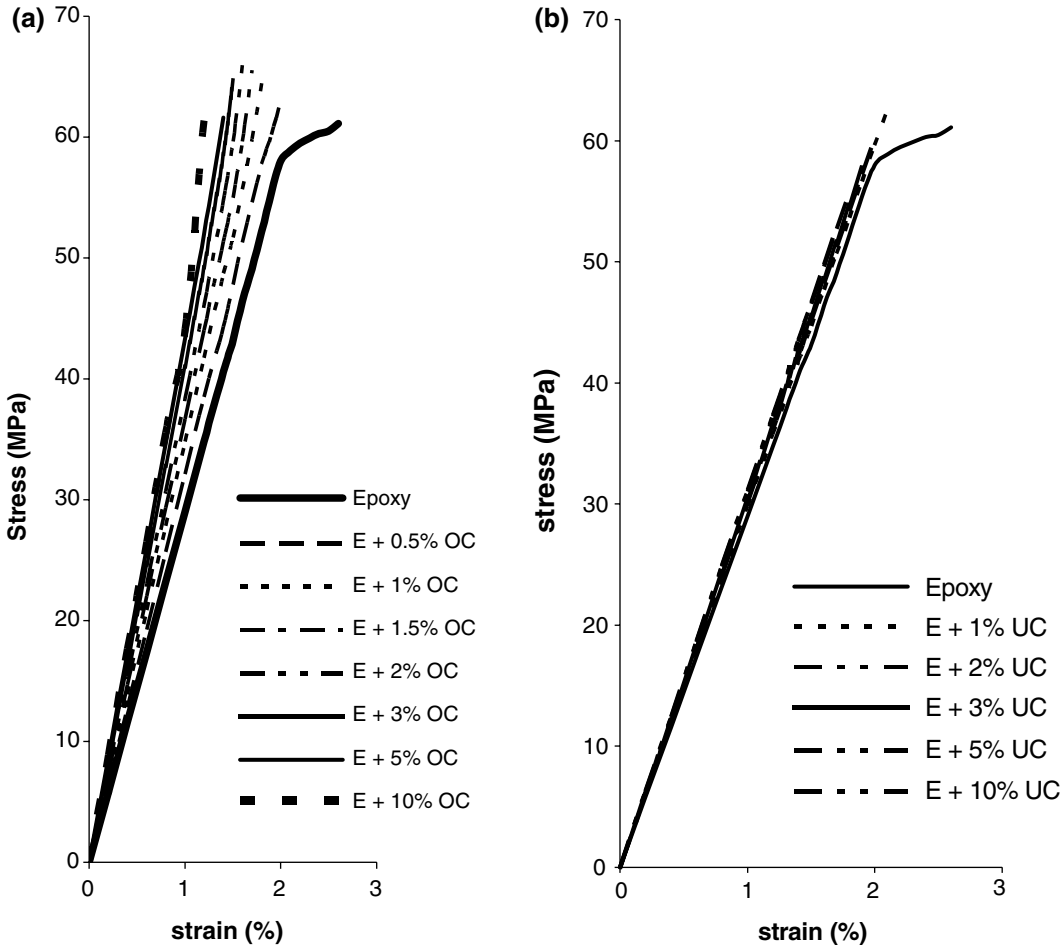

Fig. 5 Stress–strain curves of epoxy with (**a**) OC series and (**b**) UC series

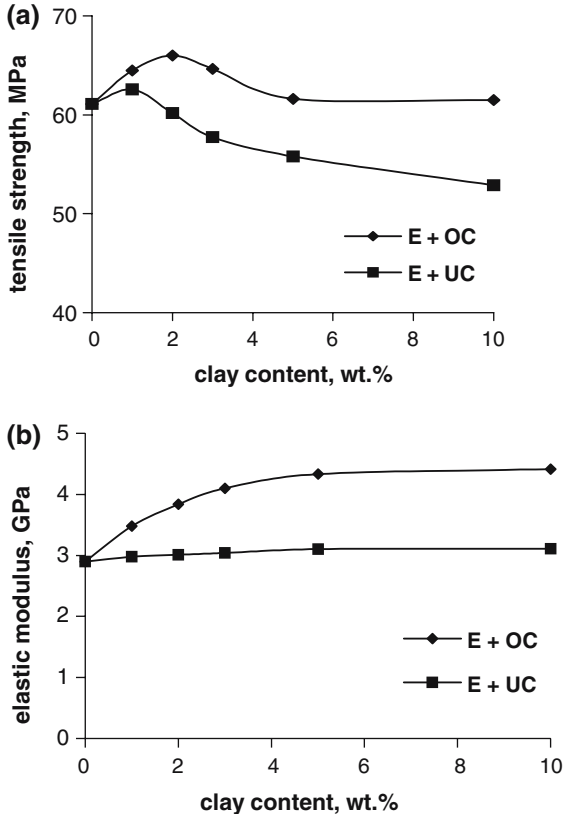

Fig. 6 Effect of clay content on (**a**) tensile strength and (**b**) tensile modulus

much improvement in modulus due to the absence of clay distribution at molecular level, and hence does not contribute to molecular strength.

The tensile fracture surfaces of epoxy and epoxy filled OC are shown in Fig. 7. Figure 8 shows the fracture surface of epoxy filled UC particles. If it seen from Fig. 7 that fracture surface of pure epoxy polymer is smooth due to brittle failure. However, on addition of OC particles, crack surface becomes rough. The roughness increases as OC content increases in the matrix. The fracture roughness indicates that the resistance of propagation of crack is large and the crack has not propagated so easily as seen in pure epoxy. The fracture surface roughness indicates that crack propagation is large and increased the torturous path of propagating crack [24]. This effect results in higher stress to failure and caused improved strength of nanocomposites. Though the fracture roughness is predominant at 10% OC, the existence of unexfolaited aggregates, voids, etc. could have decreased the strength of nanocomposites. Figure 9 shows SEM picture of epoxy with 10% OC consisting of voids. The fracture surface of epoxy with UC series is seen in Fig. 8. Fracture surface of epoxy with 1% UC is rougher than pure epoxy. At 3% UC, the presence of voids is noted. This indicates that particles have peeled off from material as crack propagates, and create void at the positions where UC particles were there. This also indicates that bonding between matrix and UC particle is poor. For higher clay content (10% UC), though the fracture surface is rough, the

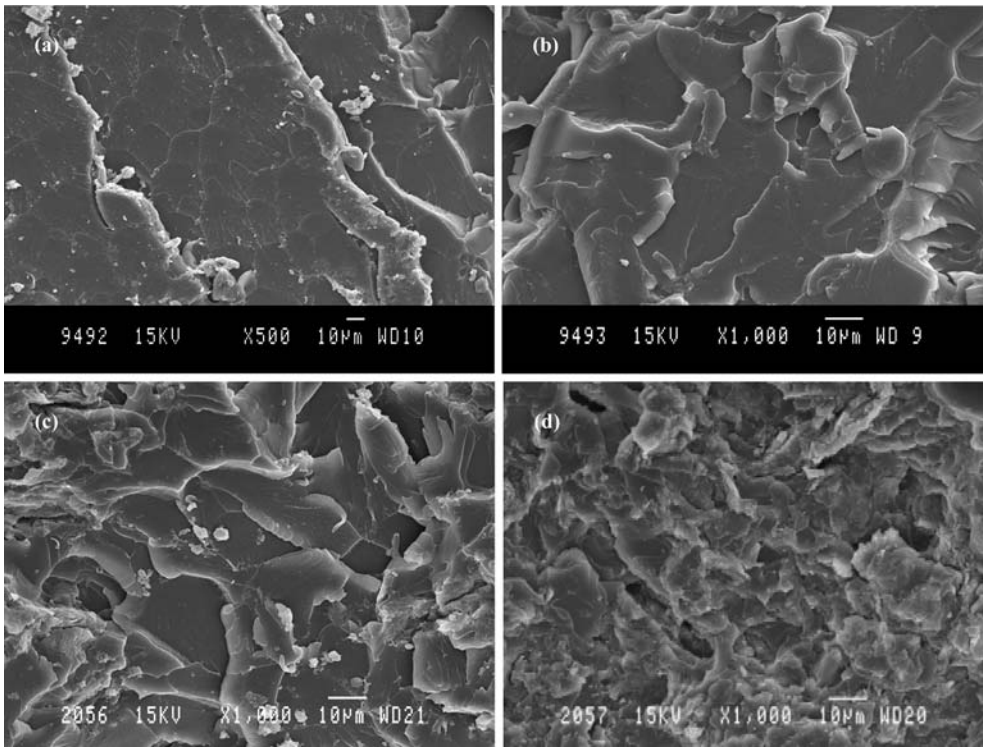

Fig. 7 SEM tensile fracture surface of (**a**) pure epoxy (**b**) E + 1% OC, (**c**) E + 3% OC and (**d**) E + 10% OC

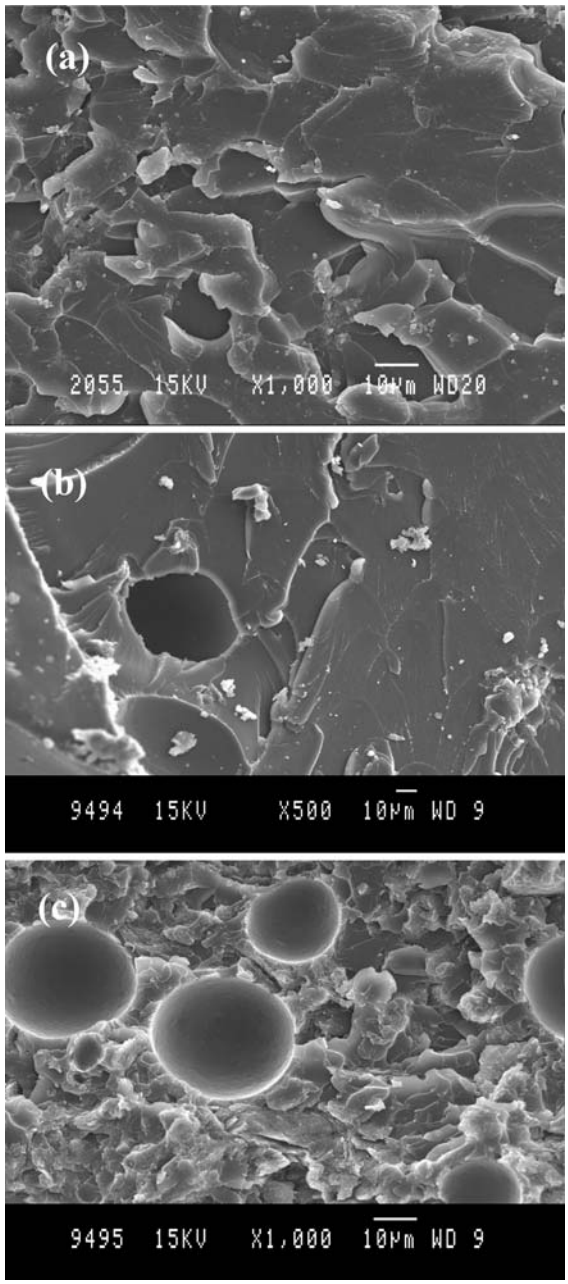

Fig. 8 SEM tensile fracture surface of (**a**) E + 1% UC, (**b**) E + 3% UC and (**c**) E + 10% UC

existence of voids is clearly visible and has decreased the strength of the material. The poor bonding strength, smooth fracture surface, voids, etc. could decrease the tensile strength of the UC filled epoxy composites. In epoxy–OC series, though the strength increases up to 2% OC, for higher clay content it decreases due to unexfoliated aggregates, voids, etc. However, the strength of nanocomposites for all clay content is higher than that of pure epoxy. It requires further investigation of the synthetic procedure to understand the methods of improving tensile strength for higher OC contents.

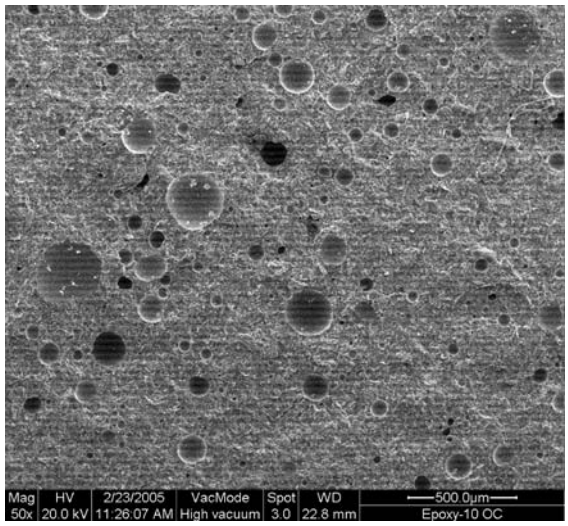

Fig. 9 SEM of epoxy + 10% OC showing the existence of voids

Impact properties

Impact results of OC and UC filled in epoxy polymer is shown in Fig. 10. It is seen that impact strength increases for values up to 3% OC and further addition of OC decreases the impact strength. The decrease in impact strength at higher filler content is due to the existence of agglomeration, unexfoliated aggregates, voids, etc. The addition of UC in epoxy decreases the impact strength of pure epoxy polymer. The impact results show that nanocomposites provide better impact properties than UC filled epoxy composites. Figure 11 shows the impact fracture surface of nanocomposites. The impact fracture surface provides the reason for impact properties in nanocomposites. Figure 11a shows that fracture surface of pure epoxy is smooth and indicates brittle failure. The addition of 1% OC, fracture surface shows rough morphology. The roughness of fracture surface increases as clay content increases (3% OC). The existence of rough surface shows that crack propagation is difficult and could have increased the torturous path and leads to high strength to failure. This

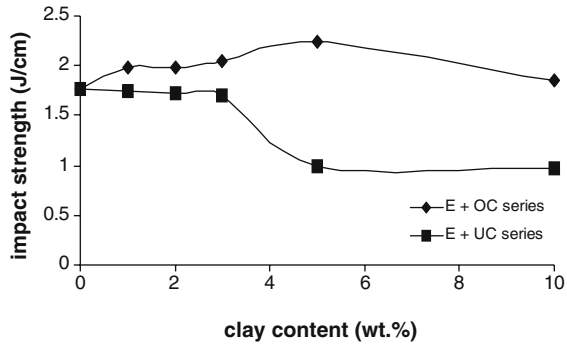

Fig. 10 Impact strength of epoxy filled with OC and UC series

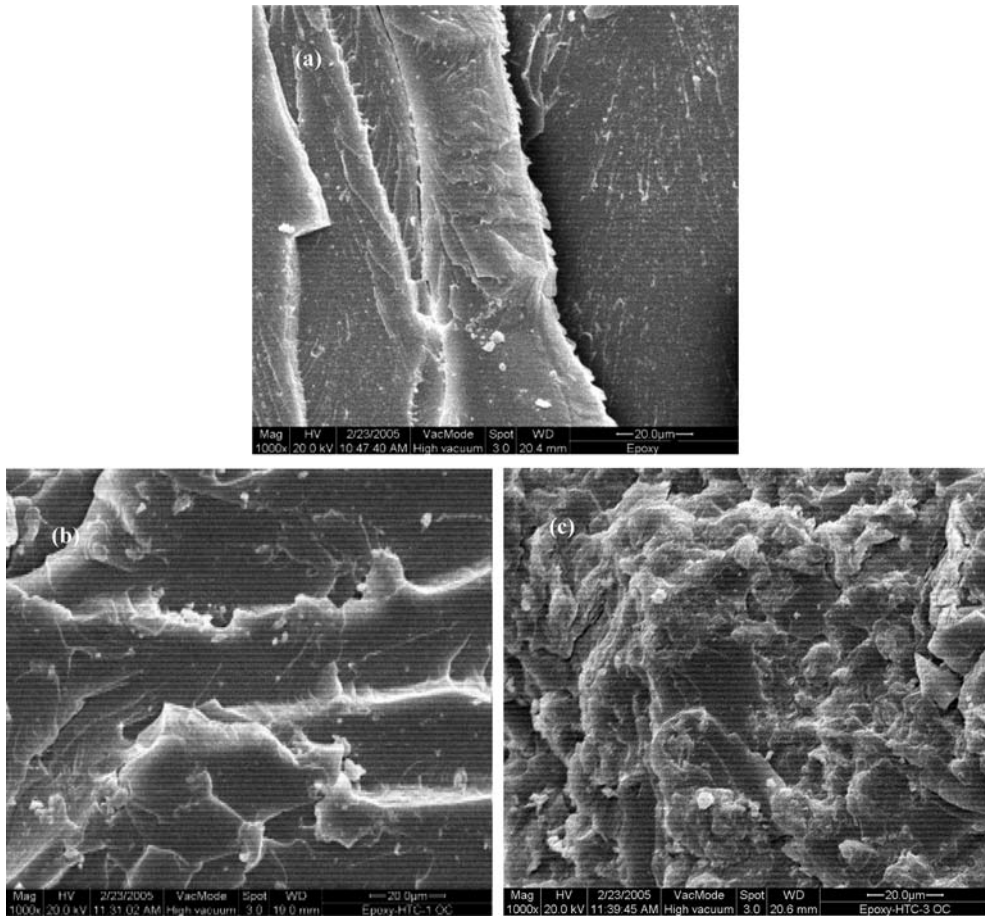

Fig. 11 SEM impact fracture surface of (**a**) pure epoxy (**b**) E + 1% OC and (**c**) E + 3% OC

has caused high impact strength of nanocomposites up to the addition of 3 wt% OC, and on higher addition. Impact results suggest that some additional energy absorbing mechanism is taking place when nano-particles are reinforced in matrix. Crack pinning, cavitation mechanisms, crack surface roughness, etc. [25] are the possible reasons for high impact strength for OC filled epoxy than that of UC filled epoxy polymer.

Vibration characteristics

Table 1 shows the effect of OC addition on natural frequency of epoxy polymer. Pure epoxy shows natural frequency of 17.87 Hz, 117.50 Hz, 191.35 Hz and 297 Hz for 1st four modes of vibrations, respectively. On addition of OC, natural frequency of all modes are higher than the epoxy polymer. For higher clay content (>3 wt%), natural frequency decreases, however higher than that of pure epoxy polymer. The large increase in stiffness due to the reinforcement of OC in the matrix causes such increased natural frequency. For higher clay content, the presence of unexfoliated aggregates of OC reduces the stiffness, which decreases the natural frequency. Table 2 shows the effect of UC addition on natural frequency of epoxy polymer. The UC addition does not improve the natural frequency of epoxy as is seen in the case of OC filler additions. A negligible effect in stiffness on reinforcement of UC in epoxy polymer matrix causes such low natural frequencies.

Figure 12 shows the effect of OC and UC addition on damping characteristics of pure epoxy polymer. Damping factors measured by LDM and IHT methods for 1st and 4th mode of natural frequencies are presented. Damping factors measured for 1st mode of natural frequencies of epoxy with OC and UC series are shown in Fig. 12a. It is observed that both the OC and UC addition increases the damping factors of pure epoxy. The OC filled epoxy increases the damping factor than that of UC filled epoxy polymer. Damping factor measured by IHT shows higher values than that of measured by LDM. The free load during impact causes increased damping in IHT. Since no free load is acting in LDM, and hence damping factor is less than that of IHT. It is seen that damping factor increases up to 3 wt% of OC, and for higher OC addition in epoxy

Table 1 Frequency dependence of epoxy and epoxy filled OC series

Material	Natural frequency at mode 1, Hz	Natural frequency at mode 2, Hz	Natural frequency at mode 3, Hz	Natural frequency at mode 4, Hz
Epoxy	17.87	117.50	191.25	297.00
E + 1% OC	18.87	134.00	205.75	305.00
E + 2% OC	20.25	135.00	216.75	327.00
E + 3% OC	22.50	148.10	233.00	332.00
E + 5% OC	18.50	128.25	229.00	317.00
E + 10% OC	18.50	123.75	221.25	308.75

Table 2 Frequency dependence of epoxy and epoxy filled UC series

Material	Natural frequency at mode 1, Hz	Natural frequency at mode 2, Hz	Natural frequency at mode 3, Hz	Natural frequency at mode 4, Hz
Epoxy	17.87	117.50	191.25	297.00
E + 1% OC	17.50	121.50	184.50	291.50
E + 2% OC	19.75	123.75	190.25	301.75
E + 3% OC	20.25	136.75	205.25	297.75
E + 5% OC	16.75	110.25	213.00	294.50
E + 10% OC	16.50	111.75	203.25	291.75

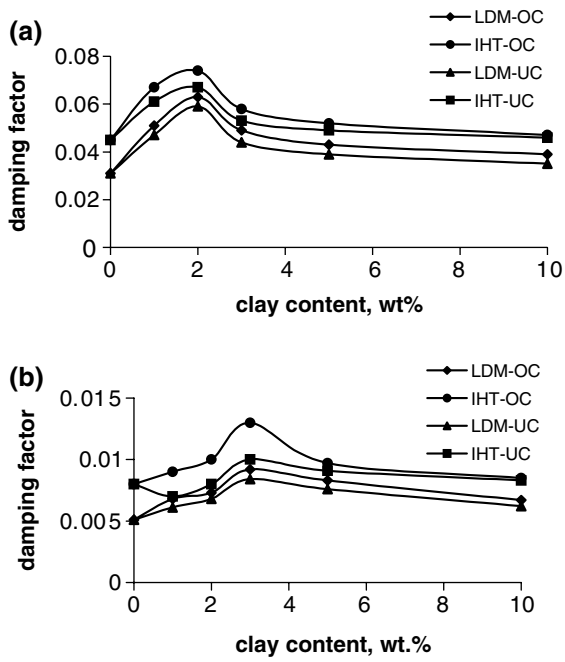

Fig. 12 Damping factor for epoxy with OC and UC series at (**a**) 1st mode and (**b**) 2nd mode

polymer, damping factor decreases but above the value of matrix material. The increased stiffness due to the addition of OC improves damping factor [26]. Similar effect in damping is noted for 4th mode of natural frequency of epoxy filled OC and UC series as shown in Fig. 12b. Though the addition of UC shows improvement in damping factor, the values are lesser than that of OC filled epoxy polymer.

Conclusions

Epoxy polymer filled with organoclays and unmodified clays are separately synthesized by adding DDM curing agent. DSC results shows that higher OC content (3% and above) leads to uneven curing and results in intercalated nanocomposite structure. The UC addition in epoxy matrix does not affect the peak exothermic curing temperature of epoxy resin. XRD shows that the formation of exfoliated nanocomposite structure up to the addition of 2 wt% OC, and for higher clay content (>2 wt%) intercalated nanocomposite structure. XRD shows that the interlayer separation is absent for unmodified clay filled in epoxy polymer and leads to micron scale filler in the epoxy polymer matrix. TEM shows the distribution of clay nanolayers at lower filler contents, and at higher clay content (10 wt%) intercalated nanocomposites is present. Tensile property of nanocomposites shows enhanced tensile modulus than that of pure epoxy resin and epoxy filled UC series. The addition of OC increases the tensile strength of epoxy polymer and UC addition decreases the tensile strength of epoxy polymer. Improved impact strength is noted for epoxy filled with OC series than those of UC filled epoxy polymer. Natural frequency of nanocomposites is higher than that of pure epoxy polymer. Damping factor is increased for epoxy/OC series than that of epoxy/UC series.

References

1. Usuki A, Kawasumi M, Kojima, Okada A (1993) J Mater Res 8:1174
2. Giannelis EP (1992) J Miner Metall Mater Soc 44:28
3. Kato M, Usuki A, Okada A (1997) J Appl Polym Sci 66:1781
4. Komarneni S (1992) J Mater Chem 2:1219
5. Pinnavaia TJ (1983) Science 220:1
6. Carrado KA (2000) Appl Clay Sci 17:1
7. Christopher Breen (1999) Appl Clay Sci 15:187
8. Velmurugan R, Mohan TP (2004) J Mater Sci 24:7333
9. Alaxandre M, Philip D (2000) Mater Sci Engg 28:1
10. Giannelis EP (1996) Adv Mater 8:29
11. Pinnavaia TJ, Beall GW (2000) Polymer–clay nanocomposites. Wiley Series in Polymer Science, New York, 127–148
12. Vaia RA, Ishi H, Giannelis EP (1993) Chem Mater 5:1674
13. Messersmith PB, Giannelis E.P (1994) Chem Mater 6:1719
14. Lan T, Pinnavaia T J (1994) Chem Mater 6:2216
15. Lan T, Kaviratna PD, Pinnavaia TJ (1995) Chem Mater 7:2144
16. Wang Z, Pinnavaia TJ (1998) Chem. Mater 10:1820
17. Butzloff P, Anne D 'Souza N, Golden TD, Garrett D (2001) Polym Eng Sci 10:1795
18. Kornmann X, Lindberg H, Berglund LA (2001) Polymer 42:1303
19. Kornmann X, Lindberg H, Berglund LA (2001) Polymer 42:4493

20. Triantafillidis CS, LeBaron PC, Pinnavaia TJ (2002) J Solid State Chem 167:354
21. Kornmann X, Thomas R, Mulhaupt R, Finter J, Berglund LA (2001) Polym Eng Sci 9l:1815
22. Yasmin Asma, Abot JL, Daniel I (2003) Scripta Mater 49:81
23. Yuan-Hsiang Yu, Ching-Yi Lin, Jui-Ming, Wei-Hsiang Lin (2003) Polymer 44:3553
24. Chun Lei Wu, Ming Qui Zhang, Min Zhi Rong, Klaus Friedrich (2002) Comp Sci Tech 62:1327
25. Wetzel B, Haupert F, Friedrich K, Zhang MQ, Rong MZ (2001) Polym Eng Sci 9:1919
26. Fornes TD, Paul DR (2003) Polymer 44:4993–5013